

Frequency Doubling, Absorption and Grating Formation in Glass Fibres: Effective Defects or Defective Effects?

P.St.J. Russell,

Physics Laboratory, University of Kent, Canterbury, U.K.,

L.J. Poyntz-Wright,

York V.S.O.P., York House, School Lane, Chandler's Ford, Hampshire, U.K.,

and D.P. Hand,

Optoelectronic Research Centre, University of Southampton, Hampshire, U.K.

Abstract The present understanding of colour centres in germanosilicate glass fibres and the diverse effects attributed to colour centre activity are reviewed. Drawing on a wide range of up-to-date research results, an attempt is made to piece together as far as possible a unified picture of the defect processes behind second harmonic generation, nonlinear transmission and photorefractive grating formation in optical fibres.

1. Introduction In recent years the role played by defects and colour centres in optical fibres has come under increasing scrutiny through the discovery of a wide variety of anomalous laser-induced effects. These range from the highly destructive (catastrophic breakdown of the fibre core – the fibre fuse^{22,28}) to the mildly annoying (gradual darkening with time and dynamic changes in transmission with intensity^{29,33}) and from the mildly useful if as yet inexplicable (second harmonic generation^{75,92,103}) to the practically important (holographic side-writing of strong permanent photorefractive gratings⁵⁶ for use in sensors, laser line-narrowing and WDM systems). The aim of this paper is to review these various effects, categorize them in terms of their usefulness or significance to a variety of fibre optics applications and perhaps even answer the question in the title.

2. Colour centres in glass Optical absorption is caused by molecular transitions involving vibrational and electronic excitations of the intrinsic glass matrix and the dopants, impurities or defects that are incorporated during glass formation. In general, electronic transitions are observed in the UV region, while molecular vibrations dominate in the IR region. In the near IR, where most optical fibres operate, the major absorption bands arise from the presence of OH bonds, but there may also be small losses from the tails of other bands which have maxima in the UV and other parts of the IR spectrum. With the increasing demand for optical fibres that perform well in the green to UV spectral range, careful optical and structural characterization of the electronic absorption bands and their influence on

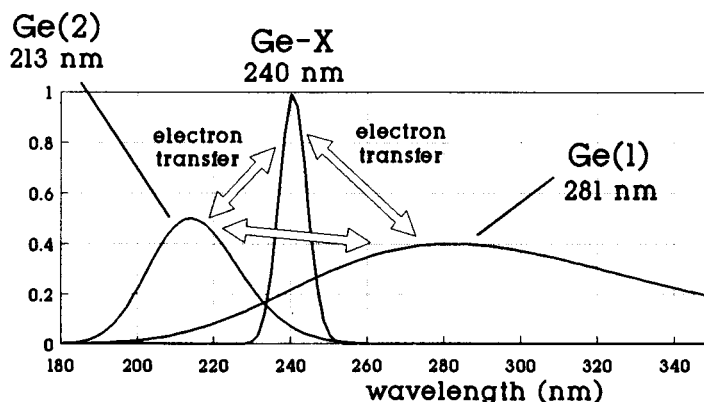


Figure 1 Absorption spectrum of GS glasses in the UV (arbitrary vertical scale). The FWHM peak widths are 0.9 eV (213 nm), 0.22 eV (240 nm) and 1.97 eV (281 nm). An additional band (not shown) exists at 325 nm whose strength scales linearly with (but $\sim 1000\times$ weaker than) the 240 nm band¹⁹. At 488 nm, two photon absorption excites and bleaches all three bands.

the transmission properties of the fibres has become important. Even in the IR, fibres that are ostensibly low loss and optically linear at moderate intensities can develop significant induced losses²⁹ and even, at high peak IR intensity levels, disallowed second order nonlinearities⁹². These effects are thought to be caused by multi-photon absorption

at electronic transitions in the UV^{15,19}. Thus, the study of colour centres in optical fibres has two main thrusts: to permit the design of fibres that may be used in low loss laser power delivery systems in the blue to UV and to explain and perhaps exploit a range of colour centre or defect-related anomalous optical effects.

Colour centres are themselves¹⁻¹⁹ the result of optically, thermally or mechanically induced microstructural changes in the glass matrix that give rise to the creation, augmentation or bleaching-out of optical absorption bands. Precursors to their formation arise through i) the dopants (for example Ge, P, Al) used to raise the core refractive index and ii) defects that form owing to inevitable non-stoichiometry and structural non-uniformities that occur during modified chemical vapour deposition (MCVD) of the core glass. Micro-clustering of the dopant species can also play a role in altering the bulk optical properties of the core material.

3. Colour centres in germanosilicate glass The germanosilicate (GS) system and its related defects – in-so far as they are relevant to the discussion – are now briefly reviewed. Germanium is the core dopant most commonly used in low-loss communications fibre, which makes it surprising and fortuitous that, in the green to ultraviolet spectral regions, GS glasses are the most photosensitive of the various alternatives. We therefore concentrate on the GS-related defects and colour centres, touching briefly on other dopants or codopants when relevant.

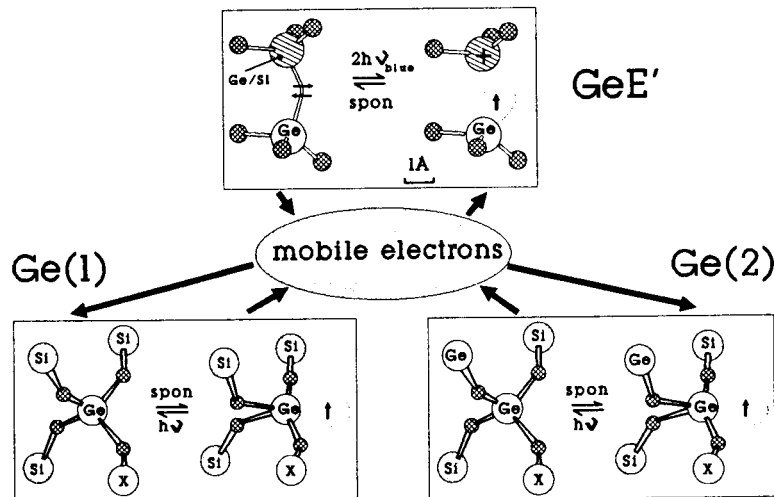
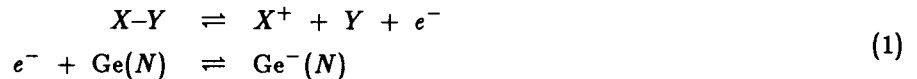


Figure 2 Proposed colour-centre model, including sketches of the individual colour centre structures (after Friebele and Griscom⁴). The identity of X in the Ge(1) and Ge(2) centres is uncertain; it may be Ge or Si. Electrons released from the Ge—X bonds by two photon absorption are trapped in Ge(1) and Ge(2) dopant sites, from which they may be released by two and single photon bleaching.

Paramagnetic centres in GS glasses have been studied extensively by ESR^{4,5,14}. Three main species have been identified – the GeE', Ge(1) and Ge(2) centres – and correlated with absorption bands in the UV (Figure 1)⁴. Widespread agreement exists over the structure of the GeE' centres^{4,17}; they consist of an unpaired electron that is localized mainly in the sp^3 orbital of a single germanium back-bonded to three neighbouring oxygens forming a trigonal pyramid (Figure 2). This was established by detection and analysis of the hyperfine ESR structure resulting from the presence of the natural isotope ^{73}Ge in the glass host (^{73}Ge is the only stable isotope of Ge that has nonzero nuclear spin $I = 9/2$)¹⁷. It is now also well established that whereas most GeE' centres are hole traps (the GeE' centre postulated by Tsai et al¹⁷ consists of an unpaired electron shared between two neighbouring Ge atoms, with a net positive charge of $+e$), the Ge(1) and Ge(2) centres are electron traps. Thus it is reasonable to suppose that the three populations are mutually supporting, i.e., the sum of the number densities of Ge(1), Ge(2) and free (i.e., untrapped) electrons equals the population of GeE' centres³³⁻³⁶. There remains some uncertainty in the literature over the precise structure of the Ge(1) and Ge(2) traps; agreement exists that they are four-coordinated Ge dopant sites substituting for Si in the glass matrix; however the identity of the four next-nearest neighbour atoms remains unclear (Figure 2). Different sources^{4,17} attribute N and $N - 1$ next-nearest neighbour Ge atoms to the ESR-identified

Ge(*N*) centres. Despite this lack of consensus, the optical spectra of the Ge(1) and Ge(2) centres have been reliably linked to unique ESR signatures. This is good enough for many purposes.

The most common type of non-stoichiometry in GS glasses formed by MCVD is oxygen deficiency, resulting in the appearance of the so-called oxygen-vacancy 'wrong-bonds' X—Y (Ge—Si, Si—Si and Ge—Ge). Routes to the formation of GeE' centres include i) breakage of these oxygen deficient bonds by direct excitation in the UV or multi-photon absorption in the blue/green/IR and ii) mechanical or thermal rupture (e.g., during fibre pulling) of the Ge—O—Ge or Si—O—Ge bonds iii) chemical reduction of these bonds by indiffusion of hydrogen. The X—Y bonds have been correlated with optical absorption bands^{1,2,3,7,19} in the vicinity of 240 nm and 320 nm. Photo-ionization releases electrons from them which migrate randomly through the glass until trapped at other sites to form Ge(1) or Ge(2) colour centres³³:



These processes are summarized in Figure 2. Notice that the tetrahedral structure around the Ge(1) and Ge(2) sites undergoes a distortion during a trapping event⁴.

It is clear that linked studies of linear optical absorption spectra and ESR are of vital importance in understanding colour centre behaviour in bulk samples. The tightly controlled exposure over very long interaction lengths that is possible in a single-mode fibre core permits measurements whose repeatability, accuracy and sensitivity would be impossible to achieve in bulk samples. However, optical characterization of the complex dynamics of the absorption induced at various laser wavelengths is also useful in providing additional information to supplement the ESR and linear absorption data. This is of particular importance in the study of nonlinear transmission.

4. Nonlinear transmission With the use of single-mode optical fibres to deliver intense blue/green radiation it has become increasingly clear that the creation of colour centres can seriously limit the system performance²⁹. Even over short time scales (minutes), the transmission (P_{out}/P_{in}) of blue/green light through single-mode GS optical fibre

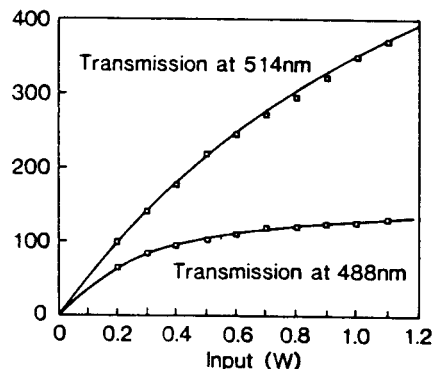


Figure 3 Transmitted power (mW) as a function of launched power at 488 nm and 514.5 nm. The full lines are fits to the model in Eq(3) – see text.

is a nonlinear function of the launched CW power level^{33,35}. Beyond a threshold of some tens of mW, the induced loss increases steadily with increasing launched power level. If the power is then reduced, the transmission recovers, but even at zero input power levels and after thermal annealing significant induced loss remains. At Ar⁺ laser wavelengths it can be an order of magnitude larger than the intrinsic absorption in unexposed fibre.

A simple phenomenological model, providing a qualitative explanation for this behaviour, may be constructed based on the idea that two photon absorption causes the creation of colour centres, while single photon absorption bleaches them out^{32,33,39,43}:

$$\frac{dn_c}{dt} = \beta h\nu n_p^2 - \sigma n_c n_p. \quad (2)$$

In this equation β is the two photon absorption constant, n_p the photon flux, n_c the colour centre population and σ their absorption (and bleaching) cross-section at optical frequency ν . In the steady-state the colour centre population is $n_{c,s} = (\beta h\nu/\sigma)n_p = (\beta/\sigma)I$, i.e., proportional to the optical intensity I . The steady-state induced absorption is $\alpha_s = \sigma n_{c,s} = \beta I$, which looks like a straightforward example of two photon absorption. This is *not* actually true (refer

to discussion below on physical basis of model). Axial variations along the fibre length may be accounted for in the steady-state by solving the equation³²:

$$dI/dz = -(\alpha_o + \beta I)I = -\alpha_o I(1 + I/I_{crit}) \quad (3)$$

where $I_{crit} = \alpha_o/\beta$ and α_o is the intrinsic absorption. This equation is easily integrable, and despite the shaky steady-state assumption impressive-looking fits can be obtained in individual cases. An example of two such fits are given in Figure 3, where one fresh 20 m length of fibre (NA=0.17, 6.5 mol% Ge) was exposed to CW 488 nm light, and another identical length to CW 514.5 light. In each case the data refers to the loss induced by a single slow upward ramp in intensity. The values of I_{crit} used for the fits were 106 mW/ μm^2 at 514.5 nm and 20 mW/ μm^2 at 488 nm, the intrinsic losses in each case being 60 dB/km and 73 dB/km respectively. The model predicts $\beta_{488} = 0.84 \text{ m}^{-1}/\text{W}\mu\text{m}^{-2}$ and $\beta_{514.5} = 0.13 \text{ m}^{-1}/\text{W}\mu\text{m}^{-2}$, which are between 10 \times and 100 \times larger than expected.

This leads us to discuss the physical basis of the model. In essence, a bistable molecular species is assumed to exist in the glass, with a 'colour centre' state that may be bleached over (by single photon absorption at blue/green wavelengths) into a second 'transparent centre' state. This state may in turn be converted (by two photon absorption) back into the colour centre state. In the steady-state at constant intensity the number densities per second of two photon events and single photon events balance, yielding an induced absorption proportional to the intensity. Elegant and appealing though it seems, this simple model is difficult to justify from what is known about the colour centres and defects that exist in the glass. For example, an electron, once released by two photon absorption from a 'wrong-bond', spends a long dwell-time as a quasi-mobile photoelectron before either getting trapped at a Ge(N) site or recombining with a GeE' centre. Thus, the population of photoelectrons is slowly augmented by two photon absorption, until it is sufficient to make the probability of GeE' recombination high enough to reach a steady-state (refer to model below). This explains the anomalously large values of β predicated by the model.

Furthermore, careful experimental measurements of the dynamics of the induced absorption show that in several respects the actual behaviour deviates embarrassingly from the predictions of the model in Eq(2), even when the steady-state assumption is discarded and both axial and temporal variations accounted for by numerical integration. For example: 1) an abrupt reduction in the intensity bleaches out the induced absorption much more slowly than predicted^{32,35}; 2) if the light is blocked abruptly after a steady state has been reached, the absorption in the fibre increases, reaching an ultimate constant level only after many hours³⁶; 3) upon relaunching light at the original power level, the absorption rapidly reverts to its previous lower level³⁶. Prolonged and detailed studies of the dynamics of

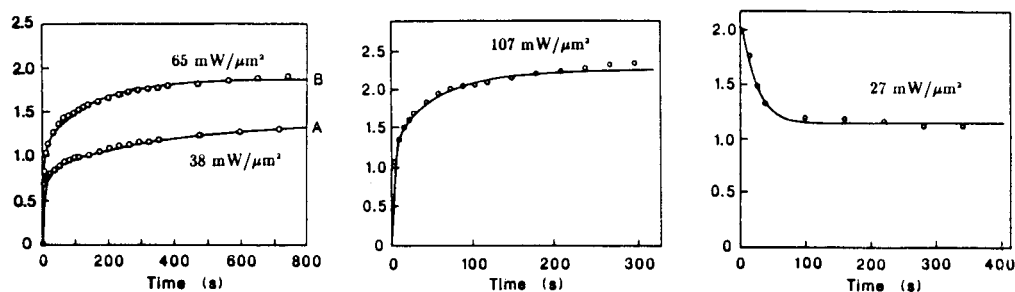


Figure 4 Dynamics of loss (dB) induced in GS fibre by CW 488 nm light. Case (c) is the behaviour seen when a high induced loss is bleached out by lowering the optical power level. The full lines are analytical fits to the complete model – see text.

the induced absorption under many different excitation conditions have provided further confirmation that this simple model is inadequate and unreliable. Hence, we chose not to present an explicit mathematical version of it in our 1988 paper³³, preferring instead to use it merely as a point of departure for the discussion. Since then a long series of careful experimental measurements has enabled us to piece together a more realistic model based on the colour centre and defect system in Figure 2. Its main assumptions are as follows:

1. Two photon absorption breaks oxygen deficient bonds, creating GeE' hole-centres and releasing electrons that drift through the glass to be trapped at Ge(1) and Ge(2) sites;

2. The resulting colour centres are bleached by two photon and single photon absorption;
3. A fraction of the GeE' hole-centre population can recombine spontaneously with free electrons; the rest are permanent.

This model predicts that the level of the induced loss will depend on the Ge dopant concentration and the degree of oxygen deficiency in the glass. Once the experimental parameters are found for a particular fibre, good fits to all kinds of intensity levels and initial conditions are obtained (see Figure 4). Experimental measurements have also shown that the induced loss in fibres pulled from a range of preforms made under standard conditions scales linearly with dopant concentration at 17 dB/km per peak $W\mu\text{m}^{-2}$ per mol% Ge (these measurements refer to exposure at 460 nm to 6 ns pulses at a repetition rate of 30 Hz)³³. Fibres pulled from oxygen-deficient preforms fabricated under reducing conditions (the presence of GeO lowers the refractive index step expected at a designed mol% of GeO₂) exhibit anomalously high induced losses.

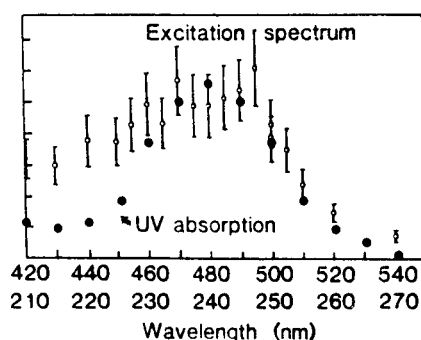


Figure 5 Excitation spectrum of the loss induced at 450 nm by different blue/green wavelengths. The level of induced absorption peaks at 480 nm, pointing to the role of two photon absorption.

The crucial role played by two photon absorption has been confirmed by measurements of the absorption induced at 450 nm by a standard exposure of fresh pieces of fibre to a range of different blue/green wavelengths. The resulting excitation spectrum (see Figure 5) peaks at 480 nm, confirming that two photon absorption to the 240 nm 'wrong-bond' band is behind the observed behaviour.

The wavelength of exposure will in general also affect the balance between two photon and single photon absorption (refer to Figure 1). In the blue/green, the induced loss is exclusively due to Ge(1) centres, whose broad absorption band centred at 281 nm extends to the near IR. For example, at 488 nm, two photon absorption will bleach out both the narrow "wrong-bond" band at 244 nm and the Ge(1) and Ge(2) bands, and single photon absorption will additionally bleach the Ge(1) band.

The spontaneous increase in absorption observed after blocking the laser light can be explained in terms of gradual retrapping of the free photo-electron population³⁶. Three characteristic exponential rates are necessary to obtain rate equation fits to the experimental data. As pointed out elsewhere, this implies that a minimum of three different species of defect centre must exist in the glass, which is encouraging in view of the known predominance of Ge(1), Ge(2) and GeE' centres.

5. Fibre fuse If the ambient temperature is raised locally around a fibre transmitting laser power, the core can be driven into thermal run-away by temperature-related increases in the optical absorption associated with colour centre formation (the rise in absorption with temperature is modelled by an Arrhenius relation with an activation energy of 2.2 eV^{22,28}). The absorption rises rapidly²¹ above about 1100°C. The result is a dramatic phenomenon known variously as the "fibre fuse" and "self-propelled self-focusing". The term "fibre-fuse" suggests a firework. This is precisely how it looks; after initial catastrophic breakdown of the core at the site of fuse initiation, an intense hot-spot propagates (fuelled by the laser light) back towards the laser at velocities of the order of 1 m/s. The term "self-propelled self-focusing" arises from the highly regular periodic damage tracks that are created^{23,27}, whose pitch is of the order of 2× the spot diameter (Figure 6). These tracks are reminiscent of those that appear in Kerr-effect self-focusing. A fundamental difference is, however, that whereas conventional self-focusing is a third-order electronic nonlinearity and hence has a very rapid time constant, the fibre-fuse (driven by thermal and optical creation of colour centres) is an energy-driven phenomenon with a relatively long time constant²². The fibre-fuse can be prevented

from wreaking havoc in high-power fibre systems by the introduction of tapers ('fuse-breakers') at sensitive points; these cause the mode spot to expand, halting the fuse by reducing the intensity below that needed for self-sustained propagation²⁰.

It can occur at quite low in-core intensity levels in the blue/green²² (as small as $5 \text{ mW}/\mu\text{m}^2$). At 1064 nm, because of the very low intrinsic absorption level, km of fibre can be destroyed²⁷. The effect has also been seen in stripe-guides of pure GeO_2 glass deposited by flame hydrolysis followed by sintering⁸³. There is evidence that the periodically-spaced damage sites are porous, containing free oxygen²⁷, perhaps through reduction from GeO_2 to GeO at the very high temperatures reached in the core (our model²² predicts 2,500 – 10,000°C).

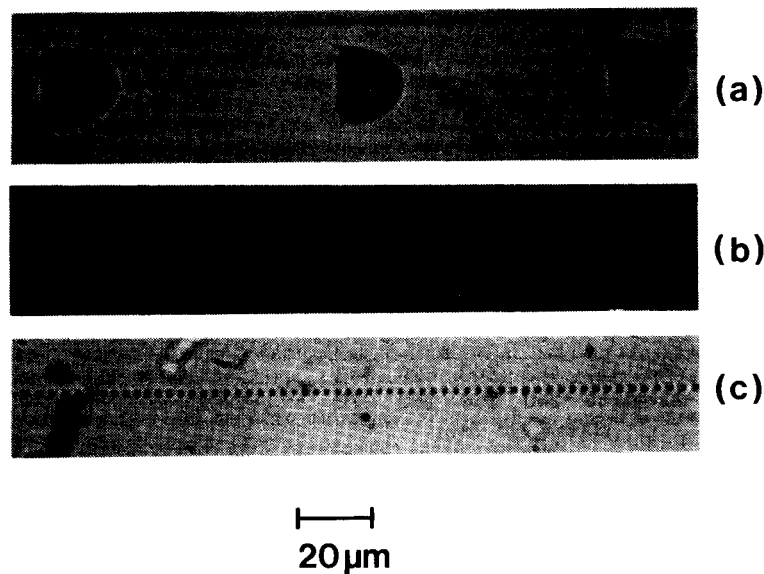


Figure 6 Examples of the damage patterns left behind after passage of the fibre fuse in (a) multimode (core diameter $40 \mu\text{m}$), (b) few-mode and (c) single mode fibres.

The velocities at which the fuse travels range from a few tens of cm/sec to several m/sec. A model based on the thermal balance between heat absorbed from the light, heat lost to the cladding, and heat left behind after passage of the fuse yields results that agree well with the experiments, confirming that Kerr-effect self-focusing plays no role. The analysis shows that the fuse may be usefully described as a thermal shock wave, and that the periodic damage tracks can be modelled by thermal lensing effects²³.

6. Refractive index changes It was back to 1978 when Hill and coworkers^{50,53} first reported that narrow-band reflection gratings could be written into standard Ge-doped silica fibres using a single-frequency Ar^+ laser at 488 and 514.5 nm. Interference of the launched light with its 4% Fresnel reflection from the remote fibre end-face (yielding interference fringes of visibility 40%) was sufficient to seed the growth of a holographic DFB grating in the fibre, with reflectivities that could approach 100%. The effect remained a curiosity for some years, due to a widespread belief that the 'Hill' fibre contained some unique and unidentifiable dopant. Since then, however, gratings have been written into a range of different single and multi-mode fibres⁴⁴⁻⁶⁸, all of which have one common feature: the presence of Ge as a core dopant. In our experiments we have found that pure silica and P-doped fibres do not produce significant index changes either with blue/green or UV light. The uniqueness of Ge is further underlined by Yin et al⁶⁸, who produced holographic gratings at 514.5 nm in thin films of sputtered GeO_2 ; they estimated an available index change of 5.2×10^{-6} .

The axial holographic process restricts the DFB operating wavelength to spectral bands where the fibre is photosensitive. These bands extend from the green to the UV (photosensitivity at very high peak Nd:YAG intensities in the 1064 nm band is too weak to be useful), outside the important spectral bands at 800, 1300 and 1550 nm. Recently, however, Meltz and coworkers⁵⁵⁻⁶⁰ have succeeded in side-writing gratings into fibres using conventional holographic interferometry and a tunable pulsed UV dye laser operating in the 240 nm 'wrong-bond' band. Their gratings are highly stable with temperature and insensitive to operating wavelengths in the near infra-red. The high *average* index

changes ($\sim 10^{-4}$) reported by Saifi et al⁶⁶ in GS fibre exposed to high intensity fsec pulses at 620 nm have also been observed by Hand et al⁴⁷⁻⁴⁹ (using a sensitive interferometric technique) at CW 514.5 and 488 nm and pulsed (6 nsec, 30 Hz) 266 nm. Not relying on a Bragg condition, this technique permits characterization of the wavelength dependence of the induced index change. It exhibits only slight dispersion with wavelength out to 1550 nm, the maximum available index change being greater than 10^{-4} regardless of the wavelength of excitation; however, the exposure needed at 266 nm is many orders of magnitude less than in the blue/green.

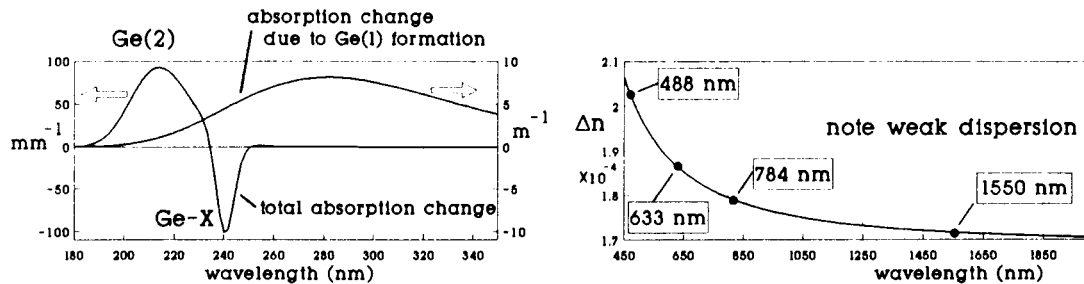


Figure 7 Differential UV absorption spectrum and resulting refractive index change (calculated using a three-term Sellmeier expansion). The points are experimental data.

The ability to produce strong distributed Bragg reflectors for use at any wavelength in standard communications fibres is an astonishing piece of luck. DBR's have many applications as strain and temperature sensors⁵⁷⁻⁶⁰ in addition to their obvious usefulness as filters for WDM systems and line-narrowing elements for single frequency operation of, for example, Er³⁺ fibre lasers at 1550 nm⁵².

7. Origin of index change Despite its proven practical importance, the physical origins of the photorefractivity are still uncertain, although significant advances have recently been made. The literature is strewn with different models. They may be divided into three classes: 1) space-charge field theories⁶⁴ inspired partly by models of photorefractivity in crystals such as Fe:LiNbO₃ and BSO, 2) Kramers-Kronig models⁴⁷ and 3) light-induced volume changes due to glass fictive temperature being very high⁶⁵. Since it has been shown that bulk index changes $> 10^{-4}$ are induced by spatially uniform light intensities^{47,48,66}, models which rely on steep spatial intensity gradients can safely be discounted as the predominant cause of the photorefractivity. This is however not to deny that photo-driven charge diffusion into Ge(1) and Ge(2) acceptor sites in the dark regions, balanced by drift in the ensuing space-charge field, may play a role; however any such role will depend on there being sufficient charge mobility in the glass matrix, something which cannot necessarily be assumed.

We have recently shown that the colour centre model proposed in the Section 4 explains quantitatively the observed index changes and their dispersion with wavelength⁴⁷. Briefly, the negative index change associated with the creation of GeE' centres is reversed by the positive index change due to Ge(2) centres, a small population of Ge(1) centres also appearing. The details of this model are available elsewhere; the differential UV absorption spectrum and the refractive index dispersion (calculated from a Sellmeier expansion over the three absorption bands) is plotted in Figure 7. The index change predicted at 1550 nm is almost as large as that predicted at 500 nm, in agreement with experimental results.

Supposing for a moment that a periodically reversing space-charge field E_{sc} were present, what effect would it have? It can easily be appreciated that the optical Kerr effect would give rise to periodic changes in refractive index at half the pitch needed to satisfy the Bragg condition. Another possibility would be the creation of an excitation-poled (see Section 8) axially-oriented $\chi^{(2)}$ which, when multiplied by E_{sc} , would yield refractive index changes; however again the resulting grating pitch is a factor of $2 \times$ too small. If, on the other hand, the supply of electron-donor centres (the 'wrong-bonds') in the bright regions were exhausted (rather like that in the lightly-doped p-side depletion region of a pn-junction with a heavily-doped n-side), E_{sc} would develop a large spatial subharmonic at the correct pitch for phase-matching. The maximum possible value of E_{sc} would occur under the (unlikely) circumstance when all the photoelectrons released by two-photon absorption diffuse into the narrow dark regions at the intensity minima (assuming high visibility fringes). It is easy to show that the axial space charge field E_{sc} increases linearly over the depletion region (populated by N' m⁻³ positively ionized GeE' hole centres), reaching a maximum value

$$\hat{E}_{sc} = (eN'\lambda/4n\epsilon_0\epsilon_r) \quad (4)$$

in the immediate vicinity of the intensity minimum. Our Kramers-Kronig model⁴⁷ (for spatially uniform illumination – see below) predicts $N' = 3.3 \times 10^{25} \text{ m}^{-3}$, which makes $\hat{E}_{sc} = 32 \text{ kV}/\mu\text{m}$ – an astonishingly high value, larger even than the breakdown field of silica ($\sim 500 \text{ V}/\mu\text{m}$). Although such fields cannot be expected in practice, it is clear that space-charge effects could play a significant role in the presence of steep intensity gradients.

That said, Kramers-Kronig effects would in fact dominate over any space-charge-related index changes because large populations of GeE' centres would be created in the bright regions while large Ge(2) and Ge(1) populations would appear in the dark regions. Large negative index changes would appear in the bright regions (bleaching out the 240 nm band) and large positive changes in the dark regions (augmenting the 217 and 281 nm bands).

A model based on third-order Kerr-effect index changes consequential to the formation of microscopic dipoles has also been proposed⁴⁷; however the number density of dipoles needed is several orders of magnitude greater than in the Kramers-Kronig model. It is also possible that light-induced density changes in the glass might play a role⁶⁵. It is well known that fused silica undergoes compaction when bombarded with energetic ion beams, causing positive index changes (the fictive temperature of the glass is very high, particularly if cooled quickly after fusing). This is unlikely to explain the effect, however, because only very small index changes can be detected in pure P-doped and undoped silica-core fibres, even when exposed to UV light at 266 and 257.3 nm.

When UV light is used to induce the index change, very high losses are induced in the blue/green⁴⁸, suggesting that a large population of Ge(1) centres is being created. It is clear that UV light will produce its own unique balance between the bleaching and trapping processes in our colour centre model – in fact favouring the creation of Ge(1) colour centres more than 488 nm or 514.5 nm light. We have obtained an induced absorption of $\alpha_{ind} = 20 \text{ dB}/\text{m}$ at 488 nm in a fibre of NA=0.3 pulled through a focused 266 nm UV beam (average power $700 \text{ W}/\text{cm}^2$, peak power $4 \text{ MW}/\text{cm}^2$) at 0.37 m/sec. Such high induced losses are clearly undesirable; however, our model predicts that exposure to blue/green light will bleach out this undesirable loss. This has been experimentally confirmed⁴⁹, the absorption induced by 266 nm light being removed by launching a mere $6 \text{ mW}/\mu\text{m}^2$ of CW Ar⁺ light at 488 nm into the fibre; the loss bleaches out from the launched end within a minute. Even more gratifying (see Figure 8), excellent numerical fits are obtained using a model that includes axial variations along the fibre and both two photon and single photon bleaching (net exponential rate given by $bI(1 + I/I_{crit}) \text{ sec}^{-1}$ with $b = 0.005 \mu\text{m}^2/\text{J}$ and $I_{crit} = 0.4 \text{ mW}/\mu\text{m}^2$).

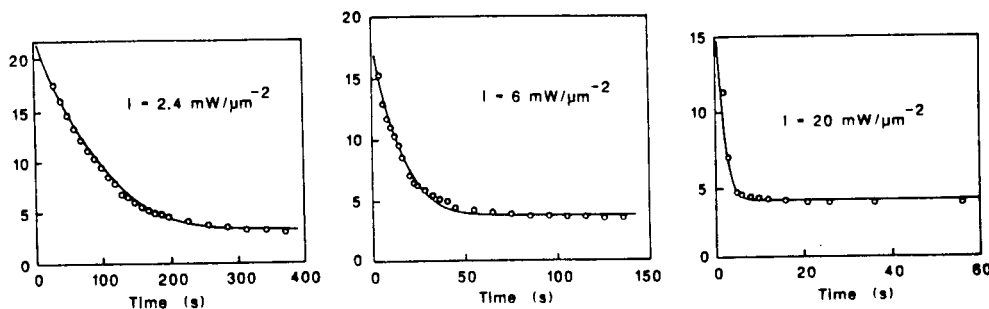


Figure 8 Dynamics of bleaching by 488 nm light (at intensities shown) in GS fibres that had been exposed from the side to 266 nm UV light. The full lines are two-parameter fits from the simple theory described in the text.

Finally, we mention the interesting observation by Parent et al⁶² that the refractive index changes written by the Hill technique are birefringent, the birefringent axes aligning with the electric field vector of the light. We would like to suggest that this is due to aligned trapping at the Ge(2) dopant sites, since these – and not the ‘wrong-bonds’ which are fixed in the glass matrix – are the only ones that a) exist in large enough numbers (according to our Kramers-Kronig model) and b) offer a choice of trapping positions. The oscillating electric field vector of the light \mathbf{E}_{opt} will cause distortions in the electronic bond structure around the Ge(2) traps, favouring the trapping of a photoelectron in one of two sites along a line running through the centre parallel to \mathbf{E}_{opt} . Non-inversion-symmetric aligned trapping at these sites may also play a role in the topic of Section 8 – second harmonic generation in fibres.

8. Second harmonic generation The observation of efficient (up to 13% has been observed at pump powers below 1 kW ⁷⁶) second harmonic generation in optical fibres was unexpected because of the macroscopic non-inversion

symmetry of the core glass and the apparent absence of any phase-matching mechanism. Such high conversion efficiencies in a readily available material raised the prospect of inexpensive green and blue laser sources, pumped by laser diodes or Q-switched fibre-lasers, and useful in a wide variety of applications. It was rapidly realized, however, that the eventual design and development of efficient fibre-based frequency doublers would depend on understanding and exploiting fully the underlying physical mechanism. This has been the main motivation for much of the effort in this area, and although some important advances have been made, much of the underlying physics remains as yet unclear.

In their original observations, Österberg and Margulis^{92,93} exposed single-mode fibre for some 10 hours to intense Q-switched mode-locked Nd:YAG pulses at 1064 nm. The second harmonic at 532 nm was observed to grow to anomalously high levels that suggested a phase-matching process. The mechanism behind the effect remained unelucidated until a spatially periodic $\chi^{(2)}$ quasi-phase-matching structure was proposed and experimentally confirmed by bandwidth measurements^{75,105} (recently a Raman scattering technique has been used to image the periodicity directly⁸²). Realizing that a dc electronic polarization or field component would possess the necessary absence of centro-symmetry, Stolen and Tom¹⁰³ identified the nonlinear rectification component

$$P_{dc}^{(3)}(K=2k_\omega - k_{2\omega}; 0=\omega + \omega - 2\omega) = \chi^{(3)} E_\omega^2 E_{2\omega}^* \quad (5)$$

as having the correct spatial period for quasi-phase-matching ($L_c = \lambda/2(n_\omega - n_{2\omega})$ where λ is the pump wavelength and n_ω and $n_{2\omega}$ the refractive indices at the pump and second harmonic frequencies¹⁰⁹). They proposed that this polarization causes self-organization or alignment of defect centres in the glass. This model has gained wide acceptance. In an elegant test of it, they seeded the process by adding a small amount of second harmonic light to the pump, and observed rapid acceleration in the rate of self-organization of the core glass, obtaining efficiencies approaching 1% after minutes instead of hours. Since the original observation, efficient frequency doubling of 1319 nm⁷⁶ and 647.1 nm¹⁰⁷ light has been reported, showing that growth in second harmonic is not strongly dependent on the wavelength of excitation.

The problem of how the process gets going in the absence of a seed (as was the case in the original experiments) was resolved by Payne⁹⁷ (see also Terhune and Weinberger¹⁰⁴). He pointed out that the tight confinement of the optical mode causes electric quadrupole moments in the core; these give rise to axially uniform second order nonlinearities from which the process can seed itself. Since it depends on the gradient of the transverse mode field, the sign of this nonlinearity reverses across the core, suggesting that the second harmonic should appear in the LP₁₁ mode, as is indeed observed. It is worth mentioning that a qualitatively similar effect will arise if there is radial diffusion of photoelectrons from the bright modal centre to Ge(N) traps in the darker annular region around the core⁶⁹. A radial space charge field E_{sc} will result, leading to an electric-field induced $\chi_{EFI}^{(2)} = 3E_{sc}\chi^{(3)}$. This would also result in self-seeding of the second harmonic into the LP₁₁ mode; however, under the correct launching conditions, the second harmonic often appears in the LP₀₁ mode in the externally seeded case, making it unlikely that space charge effects play a significant role since they would not then possess the necessary symmetry properties. Dianov et al⁷⁴ have suggested that the coherent photovoltaic effect⁷⁰ (driven by Eq(5)) might give rise to anomalously high built-in space charge fields, due to unexpected quantum corrections. This would cause an electric-field-induced second harmonic (EFISH) signal.

Laying aside the problem of the self-seeding mechanism, and accepting that all the evidence points towards defect alignment, two main questions still remain unresolved: 1) Which defects are involved and 2) How is it that a small electric polarization (typically < 1 V/cm) can align them?. In response to the question 2), Mizrahi and coworkers⁹⁰ attempted to pole a fibre preform while probing it with pulses at 1064 nm of roughly the same intensity (but a duty cycle 10⁶× smaller) as in Stolen and Tom's seeding experiments. The poling field they applied was commensurate with the estimated $P_{dc}^{(3)}$. They observed an EFISH signal, but were unable to create any permanent second order nonlinearity in the preform. In a different experiment, Bergot and coworkers⁷² subjected the core to a poling field via built-in capillary electrodes, at the same time launching blue light into it to excite the defects. This process is conveniently named *excitation poling*. Strong permanent second order nonlinearities were obtained, indicating the importance of an energetic optical pump. Another important result here is that the alignment process augments the existing EFISH signal; if the poled $\chi^{(2)}$ were caused by a built-in dc field, the SH signal would gradually diminish from its initial EFISH level as the internal field gradually cancelled out the external poling field⁹⁸. This is not observed in practice⁷².

The seeding process (which has many similarities with holography⁹⁹), by greatly accelerating the growth of the of the $\chi^{(2)}$ structure, permitted the investigation of a variety of different dopants and combinations of dopants⁷⁶. The largest effect is seen in Ge-doped glass co-doped with P. This may be because the presence of P enhances the supply of photoelectrons for subsequent trapping. However, the fact that the effect exists in many different doped glasses (very weak in pure P-doped, strongest in P/Ge co-doped, weak in pure Al-doped) means that the alignment process is not strongly species-specific.

A simple way of producing non-inversion symmetry is via changes in the local microstructure. This avoids the need for high dc fields to break the symmetry by producing the same effect through the trapping of electrons in a nonlinear field potential. In pure GS glasses we have suggested that occupied Ge(2) centres⁹⁸, which our model predicts appear in much larger numbers than Ge(1) centres⁴⁷, are responsible for $\chi^{(2)}$; these centres offer the necessary choice of at least two trapping positions that, once occupied, distort the tetrahedral Ge(2) bond angles (Figure 2). It is possible that the position in which an electron ends up can be biased by an applied poling field or an internal dc electronic polarization⁸⁵. Such a spontaneous trapping mechanism side-steps a serious problem that arises in models proposing the simultaneous excitation and alignment of an existing bond; this is the need for multiphoton excitation (two photon absorption of 532 nm light) plus the presence of a third order nonlinear alignment field ($P_{dc}^{(3)}$ of Stolen and Tom). For such a mechanism to work, these two effects must occur simultaneously, which renders the process fifth-order and therefore extremely unlikely.

It is of interest to calculate the nonlinear polarizability per occupied Ge(2) site that is needed to explain the levels of $\chi^{(2)}$ obtained experimentally in Ge-doped silica fibre. Our Kramers-Kronig model⁴⁷ predicts that in a high Ge-doped fibre $3.3 \times 10^{25} \text{ m}^{-3}$ occupied Ge(2) traps are created by exposure to blue light. The number density of molecules in crystalline LiNbO₃ is $1.88 \times 10^{28} \text{ m}^{-3}$, which implies that the Ge(2) traps are more dilute by a factor of 570 \times . The largest second order nonlinearity in LiNbO₃ is $\chi^{(2)} = 6 \times 10^{-12} \text{ m/V}$, whereas values of around 10^{-16} m/V have been induced in Ge-doped fibre. This would leave us with the result that the nonlinear polarizability of an occupied Ge(2) defect is of the order of 100 \times smaller than the value in Lithium Niobate. It is of interest to note that the dilution ratio of the aligned Ge(2) colour centres is 670 \times ; this means that actual local value of $\chi^{(2)}$ is 670 \times larger than the average value measured, predicting a local rectified optical field that is 670 \times greater than its average level. This may have implications in the alignment process.

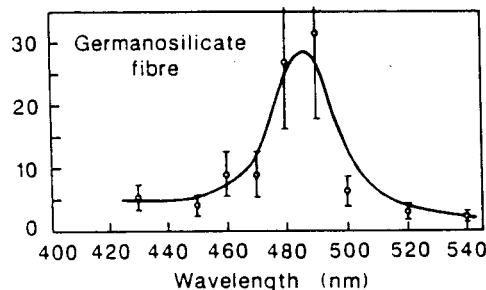


Figure 9 Excitation spectrum of second order nonlinearity induced by excitation poling at different blue/green wavelengths. The peak at 480 nm underlines the crucial role played by two photon absorption in the process.

It is unclear whether two photon absorption or second harmonic generation of the 532 nm light is the principal driving process behind defect excitation. It has been shown that the induced $\chi^{(2)}$ is bleached out by CW blue light, and that pulsed blue light bleaches it out more rapidly for the same average power^{84,96}, suggesting that two photon absorption does indeed play a role, perhaps by exciting and disorienting aligned Ge(2) traps. In GS fibres, the level of second order nonlinearity induced by excitation poling using different wavelengths in the vicinity of 480 nm (6 nsec pulses, 30 Hz repetition rate) has been investigated (Figure 9)⁸⁶. The excitation spectrum peaks at 480 nm, confirming the role played by two photon absorption into the 240 nm band. The formation of GeE' centres has also been correlated to the strength of the induced $\chi^{(2)}$ by Tsai et al¹⁰⁶.

In summary, second harmonic generation is arguably the most defective effect; it is thermally relatively unstable, will continue to evolve with time when used for frequency doubling, and is bleached by 532 nm and 488 nm light. Even so,

it is perhaps the most fascinating, and having produced 13% conversion efficiency at 950 W input power⁷⁶. is already almost interesting. As for the mechanism, there are still many unanswered questions.

9. Conclusions It can safely be concluded that the least defective effect is UV-induced refractive index changes. Here the defects are really effective; the index changes obtained are large, exhibit only slight dispersion out to 1550 nm and beyond, and are stable. Further, if one accepts the Kramers-Kronig model as the only one to explain *quantitatively* the measured index changes, then the GS system is ideal; UV-driven changes to the absorption spectrum in the UV cause refractive index changes at the wavelengths of operation, with no penalty in terms of induced absorption. The applications of strong in-core reflection gratings are too numerous to list. As for the other effects, second harmonic generation may eventually become of practical significance, provided the mechanism is elucidated. There is much scope here for exploring different glass systems, such as Pb-glasses where the nonlinear coefficients are larger. Already there are indications that in such glasses, high levels of excitation-poled second-harmonic generation can be achieved⁸⁷. Many fascinating questions remain as to the microscopic origins of the second order nonlinearity; the field is still open to new suggestions, perhaps from theorists of the curious physics of micro-clusters¹⁰⁸. As for non-linear transmission and the fibre-fuse, they are best avoided in applications unless perhaps for optical limiting. Nonlinear transmission offers a good way of accurately characterizing colour centre behaviour under different forms of optical excitation; as a unique diagnostic tool it will continue to provide valuable experimental data. Other glass systems show some promise for photorefractive fibres, and pump-excited colour centres can sometimes severely limit the performance of fibre lasers, particularly at blue/green pumping wavelengths.

References

1. Defects and colour centres

1. A.V. Amosov and S.F. Malyskin, "Role of oxygen-vacancy defects in the formation of radiation color centers in vitreous silica," *Sov.J.Glass Phys. & Chem.*, **10** (186-191) 1984.
2. A.V. Amosov and G.T. Petrovskii, "Oxygen-vacancy defects in quartz glasses", *Sov.Phys.Dokl.*, **28** (24-25) 1983.
3. A.J.Cohen and H.L.Smith, "Ultraviolet and infrared absorption of fused germania," *J.Phys.Chem.Sol.*, **7** (301-306) 1958.
4. E.J. Friebele and D.L. Griscom, "Color centers in glass optical fiber waveguides", *Mat.Res.Symp.Proc.*, **61** (319-331) 1986.
5. E.J. Friebele, D.L. Griscom and G.H. Sigel, "Defect centers in a germanium-doped silica-core optical fiber", *J.Appl.Phys.*, **45** (3424-3428) 1974.
6. E.J. Friebele, G.H. Sigel and D.L. Griscom, "Drawing induced defect centers in a fused silica core fiber," *Appl.Phys.Lett.*, **28** (516-518) 1976.
7. V. Garino-Carina, "The absorption band at 2420 Å of vitreous silica: germanium impurities and oxygen loss", *Comptes Rendues Acad.Sci. (France)*, **242** (1982-1984) 1956.
8. G.N. Greaves, "Colour centres in vitreous silica", *Phil.Mag.B*, **37** (447-466) 1978.
9. D.L. Griscom, E.J. Friebele and K.J. Long, "Fundamental defect centres in glass: Electron spin resonance and optical absorption studies of irradiated phosphorus-doped silica glass and optical fibers", *J.Appl.Phys.*, **54** (3743-3762) 1983.
10. D.L. Griscom, "Defect structure of glasses", *J.Non-Crystalline Solids*, **73** (51-77) 1985.
11. J.M. Jackson, M.E. Wells, G. Kordas, D.L. Kinser, R.A. Weeks and R.H. Magruder III, "Preparation effects on the UV optical properties of GeO₂ glasses", *J.Appl.Phys.*, **58** (2308-2311) 1985.
12. P. Kaiser, "Drawing-induced coloration in vitreous silica fibers", *J.Opt.Soc.Am.*, **64** (475-481) 1974.
13. E. O'Reilly and J. Robertson, "Theory of defects in vitreous silicon dioxide," *Phys.Rev.B*, **27** (3780-3795) 1983.
14. R.N. Schwartz, G.L. Tangonan, G.R. Blair, W. Chamulitrat and L. Kevan, "Electron paramagnetic resonance and optical study of radiation-induced defect centers in doped silica glasses", *Mat.Res.Symp.Proc.*, **61** (197-204) 1986.
15. J. Simpson, J. Ritger and F. DiMarcello, "UV-Radiation induced color centers in optical fibers," *Mat.Res.Symp.Proc.*, **61** (333-338) 1986.
16. J. Stone, "Interactions of hydrogen and deuterium with silica optical fibers: A review," *J.Lightwave Tech.*, **LT-5** (712-733) 1987.
17. T.E. Tsai, D.L. Griscom and E.J. Friebele, "On the structure of Ge-associated defect centers in irradiated high purity GeO₂ and Ge-doped SiO₂ glasses", *Diffusion and Defect Data*, **53-54** (469-476) 1987.
18. Y. Watanabe, H. Kawazoe, K. Shibuya and K. Muta, "Structure and mechanism of drawing- or radiation-induced defects in SiO₂:GeO₂ optical fiber", *Jap.J.Appl.Phys.*, **25** (425-431) 1986.
19. M.J. Yuen, "Ultraviolet absorption studies of germanium silicate glasses," *Appl.Opt.*, **21** (136-140) 1982.

2. Fibre fuse

20. D.P. Hand and T.A. Birks, "Single-mode tapers as fibre-fuse damage circuit-breakers", *Electr.Lett.*, **26** (33-35) 1990.

21. D.P. Hand and P.St.J. Russell, "Solitary thermal shock-waves and optical damage in optical fibres", Paper 10, *IEE Colloquium on Nonlinear Optical Waveguides*, (London 1988).
22. D.P. Hand and P.St.J. Russell, "Solitary thermal shock waves and optical damage in optical fibers: The fibre fuse", *Opt.Lett.*, **13** (767-769) 1988.
23. D.P. Hand and P.St.J. Russell, "Soliton-like thermal shock waves in optical fibres: Origin of periodic damage tracks", *European Conference on Optical Communications, ECOC'88*, 1988.
24. D.P. Hand, J.E. Townsend and P.St.J. Russell, "Optical damage in fibres: the Fibre Fuse", *Conference on Lasers and Electrooptics, CLEO'88*, 1988.
25. Z. Jankiewicz, M. Mindak, W. Nowakowski, J. Szyndlak and J. Wojcik, "Multimode CW Nd:YAG laser beam transmission through the fiber optic delivery system", *Optical Fibres and Their Applications IV*, SPIE **670**, (137-143) 1986.
26. M. Johnson and R.T. Hodgson, private communication, 1984.
27. R. Kashyap, "Self-propelled self-focusing damage in optical fibres", *Xth International Conf. on Lasers '87*, Paper 1509, Lake Tahoe, Nevada, Dec 1987.
28. R. Kashyap and K. Blow, "Observation of catastrophic self-propelled self-focusing in optical fibres", *Electr.Lett.*, **24** (47-48) 1988.

3. Nonlinear transmission

29. R.G.W. Brown, D.A. Jackson, J.D.C. Jones and R.K.Y. Chan, "High power fibre optic laser anemometry", ICO-13 Proceedings, Sapporo, Japan, August 1984.
30. M.C. Farries, P.R. Morkel and J.E. Townsend, "Samarium³⁺-doped glass laser operating at 651 nm", *Electr.Lett.*, **24** (709-711) 1988.
31. C.A. Miller, S.R. Mallinson, B.J. Ainslie and S.P. Craig, "Photochromic behaviour of Thulium-doped silica optical fibres", *Electr.Lett.*, **24** (590-591) 1988.
32. L.J. Poyntz-Wright, *Blue and UV Transmission in Optical Fibres*, Minitesis, University of Southampton, March 1989.
33. L.J. Poyntz-Wright, M.E. Fermann and P.St.J. Russell, "Nonlinear transmission and color-centre dynamics in germanosilicate fibers at 420-540 nm", *Opt.Lett.*, **13** (1023-1025) 1988.
34. L.J. Poyntz-Wright, M.E. Fermann and P.St.J. Russell, "Dynamics of colour-centre induced nonlinear transmission in GeO₂-SiO₂ fibres", Paper WM54, *Conference on Lasers and Electro-Optics*, Anaheim, USA, 1988.
35. L.J. Poyntz-Wright and P.St.J. Russell, "Photochromic dynamics and nonlinear transmission at modulated CW blue/green wavelengths in germanosilicate optical fibres", *Electr.Lett.*, **24** (1054-1055) 1988.
36. L.J. Poyntz-Wright and P.St.J. Russell, "Spontaneous relaxation processes in irradiated germanosilicate optical fibres", *Electr.Lett.*, **25** (478-480) 1989.
37. L.J. Poyntz-Wright and P.St.J. Russell, in preparation.
38. R.S. Taylor, K.E. Leopold, R.K. Brimacombe and S. Mihailov, "Dependence of the damage and transmission properties of fused silica fibers on the excimer laser wavelengths", *Appl. Opt.*, **27** (3124-3134) 1988.

4. Two photon absorption

39. K.W. DeLong, V. Mizrahi, G.I. Stegeman, M.A. Saifi and M.J. Andrejco, "Role of color center induced absorption in all-optical switching", *Appl.Phys.Lett.*, in press, 1990.
40. V. Mizrahi, K.W. DeLong, G.I. Stegeman, M.A. Saifi and M.J. Andrejco, "Two photon absorption as a limitation to all-optical switching", *Opt.Lett.*, **14** (1140-1142) 1989.
41. T. Mizunami and K. Takagi, "Two photon absorption of excimer-laser radiation in optical fibers", Paper ThCC17-1, *Conference on Optical Fiber Sensors* 1988.
42. A.J. Taylor, R.B. Gibson and J.P. Roberts, "Two photon absorption at 248 nm in ultraviolet window materials", *Opt.Lett.*, **13** (814-816) 1988.
43. W.T. White III, M.A. Henesian and M.J. Weber, "Photothermal lensing measurements of two photon absorption and two photon induced color-centers in borosilicate glasses at 532 nm", *J.Opt.Soc.Am. B*, **2** (1402-1408) 1985.

5. Refractive index changes

44. F.M. Durville, E.G. Brehens and R.C. Powell, "Laser-induced refractive-index gratings in Eu-doped glasses", *Phys.Rev. B*, **34** (4213-4220) 1986.
45. F.M. Durville and R.C. Powell, "Thermal lensing and permanent refractive index changes in rare-earth-doped glasses", *J.Opt.Soc.Am. B*, **4** (1934-1937) 1987.
46. D.P. Hand and P.St.J. Russell, "Single-mode fibre grating written into Sagnac loop using photosensitive fibre: Transmission filters", IOOC'89, Paper 21C3-4, Kobe, Japan, 1989.
47. D.P. Hand and P.St.J. Russell, "Photo-induced refractive index changes in germanosilicate fibres", *Opt.Lett.*, **15** (102-104) 1990.
48. D.P. Hand, P.St.J. Russell and P.J. Wells, "UV-induced refractive index changes in germaosilicate fibres", Paper F4, *Topical Meeting on Photorefractive Materials, Effects and Devices*, Aussois, France, 1990.
49. D.P. Hand, L.J. Poyntz-Wright and P.St.J. Russell, "Enhanced photorefractivity in germanosilicate fibers: effects of bleaching with 488-nm light," Paper MJ3, *Topical Meeting on Integrated Photonics Research*, Hilton Head, South Carolina, USA, March 1990.

50. K.O. Hill, Y. Fujii, D.C. Johnson and B.S. Kawasaki, "Photosensitivity in optical fiber waveguides: Application to reflection filter fabrication", *Appl.Phys.Lett.*, **32** (647-649) 1978.
51. K.O. Hill, D.C. Johnson, F. Bilodeau and S. Faucher, "Narrow-bandwidth optical waveguide transmission filters", *Electr.Lett.*, **23** (465-466) 1987.
52. R. Kashyap, J.R. Armitage, R. Wyatt, S.T. Davey and D.L. Williams, "All-fibre narrow band reflection gratings at 1500 nm", *Electr.Lett.*, **26**, (730-732) 1990.
53. B.S. Kawasaki, K.O. Hill, D.C. Johnson and Y. Fujii, "Narrow band reflectors in optical fibers", *Opt.Lett.*, **3** (66-68) 1978.
54. D.K.W. Lam and B.K. Garside, "Characterisation of single-mode optical fiber filters", *Appl.Opt.*, **20** (440-445) 1981.
55. G. Meltz, J.R. Dunphy, W.H. Glenn, J.D. Farina and F.J. Leonberger, Paper 14, SPIE **798**, The Hague, Holland, 1987.
56. G. Meltz, W.W. Morey and W.H. Glenn, "Formation of Bragg gratings in optical fibers by a transverse holographic method", *Opt.Lett.*, **14** (823-825) 1989.
57. G. Meltz, W.W. Morey, W.H. Glenn and J.D. Farina, "In-fiber Bragg grating sensors", *Topical Meeting on Optical Fiber Sensors*, Paper ThBB5, 1988.
58. G. Meltz, W.W. Morey and W.H. Glenn, "In-fiber Bragg grating tap", *Conference on Optical Fiber Communications, OFC'90*, San Francisco, California, 1990.
59. W.W. Morey, G. Meltz and W.H. Glenn, "Bragg-grating temperature and strain sensors", *Springer Proceedings in Physics*, **44** (526-531) 1989.
60. W.W. Morey, G. Meltz and W.H. Glenn, "Fiber optic Bragg grating sensors", *Fiber Optical and Laser Sensors VII*, Paper 1169-12, SPIE **1169**, Boston, Mass., 1989.
61. F. Oulette, "Phase-matching of optical fibre photorefractive intermodal couplers in infra-red", *Electr.Lett.*, **25** (1590-1592) 1989.
62. M. Parent, J. Bures, S. Lacroix and J. Lapierre, "Propriétés de polarisation des réflecteurs de Bragg induits par photosensibilité dans les fibres optiques monomodes", *Appl.Opt.*, **24** (354-357) 1985.
63. H.G. Park and B.Y. Kim, "Intermodal coupler using permanently photoinduced grating in two-mode optical fibers", *Electr.Lett.*, **25** (797-799) 1989.
64. F.P. Payne, "Photorefractive gratings in single-mode optical fibres", *Electr.Lett.*, **25** (498-499) 1989.
65. M. Rothschild, D.J. Erlich and D.C. Shaver, "Effects of excimer laser radiation on the transmission, index of refraction and density of ultraviolet grade fused silica", *Appl.Phys.Lett.*, **55** (1276-1278) 1989.
66. M.A. Saifi, Y. Silberberg, A.M. Weiner, H. Fouckhardt and M.J. Andrejco, "Sensitivity of dual-core fiber coupler to light-induced defects", *Phot.Tech.Lett.*, **1** (386-388) 1989.
67. J. Stone, "Photorefractivity in GeO₂-doped silica fibers", *J.Appl.Phys.*, **62** (4371-4374) 1987.
68. Z.Y. Yin, P.E. Jessop and B.K. Garside, "Photoinduced grating filters in GeO₂ thin-film waveguides", *Appl.Opt.*, **22** (4088-4092) 1983.

6. Second harmonic generation

69. D.Z. Anderson, "Efficient second-harmonic generation in glass fibers: The possible role of photo-induced charge redistribution", *Nonlinear optical properties of materials*, SPIE **1148** (186-196) 1989.
70. É.M. Bashkin and M.V. Éntin, "Coherent photovoltaic effect due to the quantum corrections", *JETP Lett.*, **48** (601-604) 1989.
71. B. Batdorf, C. Krautschik, U. Österberg, G. Stegeman, J.W. Leitch and J.R. Rotgé, "Study of length dependence of frequency doubled light in optical fibres", *Opt.Commun.*, **73** (393-397) 1989.
72. M.-V. Bergot, M.C. Farries, M.E. Fermann, L. Li, L.J. Poyntz-Wright, P.St.J. Russell and A. Smithson, "Generation of permanent optically-induced second-order nonlinearities in optical fibres by poling", *Opt.Lett.*, **13** (592-594) 1988.
73. Y. Chen, "Frequency doubling in weakly guiding optical fibers," *Appl.Phys.Lett.*, **54** (1195-1197) 1989.
74. E.M. Dianov, P.G. Kazansky, D.Yu. Stepanov and V.B. Sulimov, "Photovoltaic mechanism of photoinduced second harmonic generation in optical fibers," Paper MJ1, *Topical Meeting on Integrated Photonics Research*, Hilton Head, South Carolina, USA, March 1990.
75. M.C. Farries, P.St.J. Russell, M.E. Fermann and D.N. Payne, "Second harmonic generation in an optical fibre by self-written $\chi^{(2)}$ grating," *Electron.Lett.*, **23** (322-323) 1987.
76. M.C. Farries, "Efficient second harmonic generation in an optical fibre", Paper 20, *IEE Colloquium on Nonlinear Optical Waveguides*, (London 1988).
77. M.C. Farries and M.E. Fermann, "Frequency doubling of 1.319 μm radiation in an optical fibre by optically written $\chi^{(2)}$ grating", *Electr.Lett.*, **24** (294-295) 1988.
78. M.E. Fermann, M.C. Farries, P.St.J. Russell and L.J. Poyntz-Wright, "Tunable holographic second-harmonic generators in high-birefringence optical fibers", *Opt.Lett.*, **13** (282-284) 1988.
79. M.E. Fermann, L.Li, M.C. Farries, L.J. Poyntz-Wright and L. Dong, "Second-harmonic generation using gratings optically written by mode interference in poled optical fibres," *Opt.Lett.*, **14** (748-750) 1989.
80. M.E. Fermann, L.Li, M.C. Farries and D.N. Payne, "Frequency doubling by modal phase-matching in poled optical fibres", *Electr.Lett.*, **24** (894-895) 1988.

81. Y. Fujii, B.S. Kawasaki, K.O. Hill and D.C. Johnson, "Sum-frequency light generation in optical fibers," *Opt.Lett.*, **5** (48-50) 1980.
82. A. Kamal, D.A. Weinberger and W.H. Weber, "Spatially resolved Raman study of self-organized $\chi^{(2)}$ gratings in optical fibers", *Opt.Lett.*, **15** (613-615) 1990.
83. R. Kashyap, B.J. Ainslie and G.D. Maxwell, "Second harmonic generation in GeO₂ ridge waveguide", *Electr.Lett.*, **25** (206-208) 1989.
84. A. Krotkus and W. Margulis, "Investigations of the preparation process for efficient second-harmonic generation in optical fibers", *Appl.Phys.Lett.*, **52** (1942-1944) 1988.
85. B. Lesche, "Microscopic model of second-harmonic generation in glass fibers," *J.Opt.Soc.Am. B*, **7** (53-56) 1990.
86. L. Li and M.E. Fermann, "Poling techniques for optical fibres," *Quantum Electronics and Laser Science Conference*, Paper FCC1, Baltimore, Maryland, U.S.A., April 1989.
87. L. Li, P.J. Wells, E.R. Taylor and D.N. Payne, "Generation of permanent second-order susceptibility in lead-silicate fibres," Paper MJ5, *Topical Meeting on Integrated Photonics Research*, Hilton Head, South Carolina, USA, March 1990.
88. W. Margulis, I.C.S. Carvalho and J.P. von der Weid, "Phase measurement in frequency-doubling fibers", *Opt.Lett.*, **14** (700-702) 1989.
89. W. Margulis and U. Österberg, "Second-harmonic generation in optical glass fibers", *J.Opt.Soc.Am. B*, **5** (312-315) 1988.
90. V. Mizrahi, U. Österberg, J.E. Sipe and G.I. Stegeman, "Test of a model of efficient second-harmonic generation in glass optical fibers", *Opt.Lett.*, **13** (279-282) 1988.
91. T. Nakashima, M. Nakazawa, Y. Negishi, "Sum-Frequency Generation in a Polarization-Preserving Optical Fiber," *Jap.J.Appl.Phys.*, **24** (L308-L310) 1985.
92. U. Österberg and W. Margulis, "Dye laser pumped by Nd:YAG laser pulses frequency doubled in a glass optical fiber", *Opt.Lett.*, **11** (516-518) 1986.
93. U. Österberg and W. Margulis, "Experimental studies on efficient frequency doubling in glass optical fibers", *Opt.Lett.*, **12** (57-59) 1987.
94. U. Österberg, "Growth of third-harmonic signal in optical glass fibre", *Electr.Lett.*, **26** (103-104) 1990.
95. F. Oulette, K.O. Hill and D.C. Johnson, "Enhancement of second-harmonic generation in optical fibers by hydrogen and heat treatment," *Appl.Phys.Lett.*, **54** (1086-1088) 1989.
96. F. Oulette, K.O. Hill, D.C. Johnson, "Light-induced erasure of self-organized $\chi^{(2)}$ gratings in optical fibers," *Opt.Lett.*, **13** (515-517) 1988.
97. F.P. Payne, "Frequency-doubling in single mode optical fibres", *Electr.Lett.*, **23** (1215-1217) 1987.
98. L.J. Poyntz-Wright and P.St.J. Russell, "A colour-centre model for second-order optical nonlinearities in germanosilicate optical fibres," Paper MJ4, *Topical Meeting on Integrated Photonics Research*, Hilton Head, South Carolina, USA, March 1990.
99. P.St.J. Russell, "Nonlinear holography for wavefront conversion, frequency doubling and parametric amplification," Paper WC5, *Topical Meeting on Integrated Photonics Research*, Hilton Head, South Carolina, USA, March 1990.
100. M.A. Saifi and M.J. Andrejco, "Second-harmonic generation in single-mode and multimode fibers," *Opt.Lett.*, **13** (773-775) 1988.
101. Y. Sasaki and Y. Ohmori, "Phase-matched sum-frequency light generation in optical fibers," *Appl.Phys.Lett.*, **39** (466-468) 1981.
102. M.D. Selker and N.M. Lawandy, "Temperature sensitivity of seeded second harmonic generation in germanosilicate optical fibres," *Electr.Lett.* **25** (1440-1442) 1989.
103. R.H. Stolen and H.W.K. Tom, "Self-organized phase-matched harmonic generation in optical fibers", *Opt.Lett.*, **12** (585-587) 1987.
104. R.W. Terhune and D.A. Weinberger, "Second-harmonic generation in fibers", *J.Opt.Soc.Am. B*, **4** (661-674) 1987.
105. H.W.K. Tom, R.H. Stolen, G.D. Aumiller and W. Pleibel, "Preparation of long-coherence-length second-harmonic-generating optical fibers by using mode-locked pulses", *Opt.Lett.*, **13** (512-514) 1988.
106. T.E. Tsai, M.A. Saifi, E.J. Friebele, D.L. Griscom and U. Österberg, "Correlation of defect centers with second-harmonic generation in Ge-doped and Ge-P-doped silica-core single-mode fibers," *Opt.Lett.*, **14** (1023-1025) 1989.
107. B. Valk, E.M. Kim and M.M. Salour, "Second harmonic generation in Ge-doped fibers with a mode-locked Kr⁺ laser", *Appl.Phys.Lett.*, **51** (722-724) 1987.

7. Miscellaneous

108. M.A. Duncan and D.H. Rouvray, "Microclusters", *Scientific American*, December 1989 (110-115).
109. J.W. Fleming, "Dispersion in GeO₂-SiO₂ glasses", *Appl.Opt.*, **23** (4486-4493) 1984.